Open
ORIGINAL ARTICLE

Cell Research (2013) 23:351-365.
© 2013 IBCB, SIBS, CAS All rights reserved 1001-0602/13
www.nature.com/cr

β-Arrestin1 regulates γ-secretase complex assembly and modulates amyloid-β pathology

Xiaosong Liu[1, *], Xiaohui Zhao[1, *], Xianglu Zeng[1], Koen Bossers[3], Dick F Swaab[3], Jian Zhao[1, 2], Gang Pei[1, 2, 4]

[1]State Key Laboratory of Cell Biology, Institute of Biochemistry and Cell Biology, Shanghai Institutes for Biological Sciences, Chinese Academy of Sciences, [2]Graduate School of the Chinese Academy of Sciences, Shanghai 200031, China; [3]Netherlands Institute for Neuroscience, Meibergdreef 47, 1105 BA Amsterdam, The Netherlands; [4]School of Life Science and Technology, Tongji University, Shanghai 200092, China

Alzheimer's disease (AD) is a progressive and complex neurodegenerative disease in which the γ-secretase-mediated amyloid-β (Aβ) pathology plays an important role. We found that a multifunctional protein, β-arrestin1, facilitated the formation of NCT/APH-1 (anterior pharynx-defective phenotype 1) precomplex and mature γ-secretase complex through its functional interaction with APH-1. Deficiency of β-arrestin1 or inhibition of binding of β-arrestin1 with APH-1 by small peptides reduced Aβ production without affecting Notch processing. Genetic ablation of β-arrestin1 diminished Aβ pathology and behavioral deficits in transgenic AD mice. Moreover, in brains of sporadic AD patients and transgenic AD mice, the expression of β-arrestin1 was upregulated and correlated well with neuropathological severity and senile Aβ plaques. Thus, our study identifies a regulatory mechanism underlying both γ-secretase assembly and AD pathogenesis, and indicates that specific reduction of Aβ pathology can be achieved by regulation of the γ-secretase assembly.

***Keywords*:** Alzheimer's disease; β-arrestin1; APH-1; γ-secretase

Cell Research (2013) **23**:351-365. doi:10.1038/cr.2012.167; published online 4 December 2012

Introduction

Alzheimer's disease (AD) is a progressive neurodegenerative disorder and the most common form of dementia, accounting for 50%-70% percent of worldwide dementia cases [1]. The major sporadic AD cases exhibit onset in their 70s or even later, whereas the minor, mutation linked, familial AD cases exhibit onset typically during their 50s [2, 3]. Most cases of AD suffer from neuron loss, synaptic dysfunction, cognitive impairment and inability to function independently [1, 4, 5]. Decades of researches have pathologically characterized AD by two proteinaceous aggregates: amyloid plaques composed of amyloid-β (Aβ) peptides [6] and neurofibrillary tangles consisting of the hyperphosphorylated microtubule-associated protein tau [7]. The Aβ peptides are products of sequential processing of amyloid-β precursor protein (APP) by BACE (β-amyloid cleaving enzyme) and γ-secretase complex, comprising at least presenilin (PS), nicastrin (NCT), anterior pharynx-defective phenotype 1 (APH-1) and presenilin enhancer 2 (PEN-2) [8-10].

Although the etiologies of most sporadic AD cases are still elusive, considerable researches have demonstrated that the G protein-coupled receptors (GPCRs) are involved. In 2004, Blalock *et al*. [11] reported a gene expression profile of AD patients' postmortem brains by cDNA microarray analysis, showing that the levels of transcripts from a number of GPCR genes changed, among which were inflammation-associated GPCRs (e.g., leukotriene B4 receptor, histamine receptor H3), hormone receptors (e.g., angiotensin II receptor, parathyroid hormone receptor 1), neurotransmitter receptors (dopamine receptor D2, D4, gamma-aminobutyric acid B receptor 1), orphan GPCRs (GPR17, GPR22, GPR55) and some others (e.g., purinergic receptor P2Y G-protein-coupled 10, sphingolipid G protein-coupled

*These two authors contributed equally to this work.
Correspondence: Gang Pei[a], Jian Zhao[b]
[a]E-mail: gpei@sibs.ac.cn
[b]E-mail: jzhao@sibs.ac.cn
Received 12 July 2012; revised 27 September 2012; accepted 28 October 2012; published online 4 December 2012

receptor 1). Recent studies have revealed that the sequential processing of APP by BACE and γ-secretase can be directly regulated by GPCRs, including δ-opioid receptor (DOR) [12], β_2-adrenergic receptor (β_2AR) [13] and the orphan GPR3 [14]. Moreover, the CCR2, a chemokine GPCR expressed on microglia, has been demonstrated to play a protective role in the early stages of AD pathogenesis by promoting Aβ clearance [15]. All these investigations suggest a potential role of GPCRs in the pathological progression of AD.

Bossers *et al*. [16] have used a large set of well-characterized PFC samples to identify gene expression profiles in sporadic AD patients' brains. They reported several clusters of genes with concerted alterations over the consecutive Braak stages and their possible involvement in AD pathogenesis. Intriguingly, they found that the most profound changes occur just before the onset of senile plaque pathology, suggesting that disturbances in this balance might cause a positive feedback loop where increasing levels of neuronal activity are paralleled by a buildup of Aβ. Interestingly, a set of proteins involved in signaling pathways have been shown to be altered in expression in their study. β-Arrestin1 is one of the signaling mediator and scaffolding protein that has been found to be upregulated.

It is well known that after stimulation by ligand, the GPCRs undergo desensitization and internalization mediated by the multifunctional adaptor proteins called arrestins [17]. Recruitment of arrestins sterically hinders further G protein coupling to the GPCR, thereby leading to desensitization of GPCRs and even mediating a G protein-independent signaling pathway [18]. The arrestin family includes four members: arrestin1 (visual arrestin), arrestin2 (β-arrestin1), arrestin3 (β-arrestin2) and arrestin4 (cone arrestin). While the arrestin1/4 are localized only in the retinal rods and cones, the arrestin2/3 (β-arrestin1/2) are expressed ubiquitously [19]. The β-arrestin1 is expressed especially higher in CNS (central nervous system) (THE HUMAN PROTEIN ATLAS, http://www.proteinatlas.org). In light of the recently identified roles of GPCRs in the AD pathogenesis as well as the potential correlation of β-arrestins with AD pathogenesis, this study is aimed to further elucidate the potential regulatory mechanisms of β-arrestins in AD progression.

Results

β-Arrestin1 modulates Aβ production and γ-secretase activity

To test whether β-arrestin1 plays a role in AD pathogenesis, we measured the endogenous Aβ levels in β-arrestin1-knockout mouse brains. We found that the endogenous Aβ40 and Aβ42 production were reduced in hippocampus and cortex of β-arrestin1-knockout mouse brains (Figure 1A). Furthermore, western blot analysis of the mouse brain samples revealed that β-arrestin1 deficiency resulted in the accumulation of both amyloidogenic (CTFβ, C99) and non-amyloidogenic (CTFα, C83) carboxyl-terminal APP fragments without altering the levels of full-length APP (Figure 1B). Because both C99 and C83 are immediate substrates of γ-secretase, these results suggest that the elimination of β-arrestin1 might alter γ-secretase activity and APP processing, thereby contributing to the reduced Aβ levels in β-arrestin1-knockout mice. Thus, we measured the activities of α-, β- and γ-secretase in these mouse brain samples. We found that the activity of γ-secretase but not that of α- or β-secretase was significantly reduced in β-arrestin1-knockout mice compared with that in the wild-type mice (Figure 1C), suggesting a downregulation of γ-secretase activity. Consistent with these results, we found that suppression of β-arrestin1 expression by specific siRNA reduced Aβ40 and Aβ42 production and γ-secretase activity in both primary neurons (Figure 1D) and Neuro-2a neuroblastoma cells (Supplementary information, Figure S1A). Conversely, β-arrestin1 overexpression increased Aβ40 and Aβ42 production and γ-secretase activity in both primary neurons (Figure 1E) and Neuro-2a neuroblastoma cells (Supplementary information, Figure S1B). In contrast, altered β-arrestin1 level failed to affect either α- or β-secretase activities (Supplementary information, Figure S1A and S1C). We found that the activities of neprilysin and insulin degrading enzyme, which degrade Aβ, were not affected by changes in the β-arrestin1 level (data not shown). To directly monitor the γ-secretase activity, the *in vitro* C99 assay was performed. We purified C99 peptide from Hi-5 insect cells. Equal amount of cell microsomal membrane fractions were then incubated with C99 peptide, and the *de novo* generated AICDs (APP intracellular domains) were monitored. As shown in Figure 1F, significantly more AICD was generated when microsomal membrane fractions from the cells overexpressing β-arrestin1 were applied, indicating that the elevation of β-arrestin1 expression enhanced γ-secretase activity. Collectively, these data suggest that expression of β-arrestin1 contributes to the enhanced Aβ production and γ-secretase activity.

β-Arrestin1 enhances γ-secretase activity via its interaction with APH-1

By interacting with diverse signaling proteins, β-arrestin1 mediates the formation of signaling protein complexes and activation of downstream kinase cascades

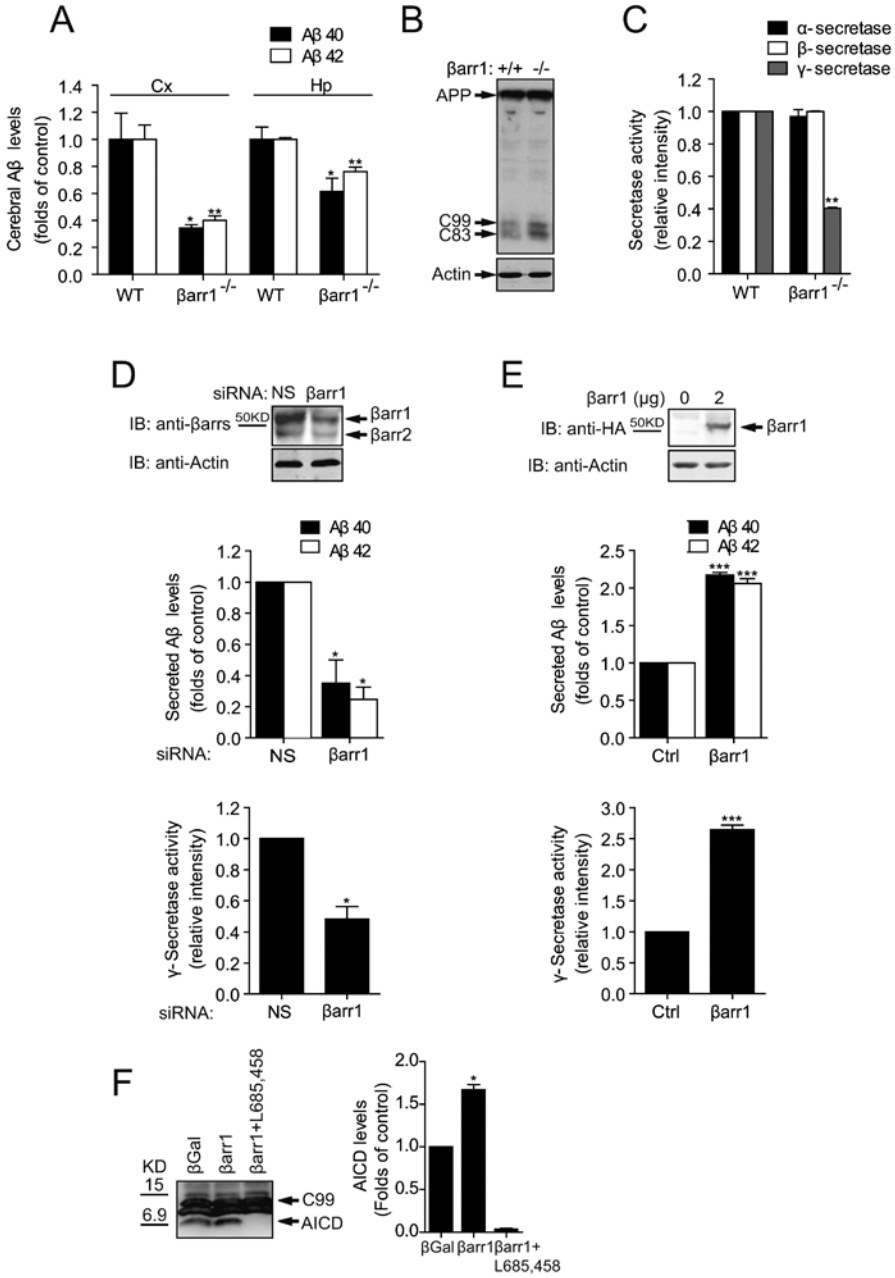

Figure 1 β-Arrestin1 modulates Aβ production and γ-secretase activity. **(A)** β-arrestin1 modulates endogenous Aβ production in non-AD mice. Cortical (Cx) and hippocampal (Hp) levels of Aβ40 and Aβ42 in wild-type (WT) and β-arrestin1-knockout ($\beta arr1^{-/-}$) mice (*n* = 4-5 for each group) were measured by ELISA. **(B)** Full-length APP and APP fragments in the hippocampal extracts from β-arrestin1-knockout mice. Protein extracts were subjected to western blot using antibodies against APP and actin. **(C)** Activities of α-, β-, and γ-secretase in hippocampal extracts of WT and $\beta arr1^{-/-}$ mice were measured by specific fluorogenic substrate assay (*n* = 4 for each group). Data are shown as mean ± SEM of at least three independent experiments. **(D)** Mouse primary neurons were transfected with β-arrestin1 specific siRNA or non-specific control siRNA and were cultured for 7 days (upper panel). Secreted Aβ levels (middle panel) were measured by ELISA and γ-secretase activity (lower panel) was measured by specific fluorogenic substrate assay. **(E)** Mouse primary neurons were transfected with vectors carrying HA-tagged human β-arrestin1 cDNA or control vectors (upper panel). 48 h after transfection, secreted Aβ levels and γ-secretase activity were measured as **(D)**. Data are shown as mean ± SEM of at least three independent experiments. **P* < 0.05, ***P* < 0.01, ****P* < 0.001. NS, non-specific oligomer; Ctrl, control. **(F)** C99 γ-secretase assay. Equal amount of microsomal membrane fractions of HEK293T cells overexpressing βGal or human β-arrestin1 was subjected to *in vitro* γ-secretase assay using purified C99. γ-secretase activity was reflected by production of AICDs. Specificity of the reaction was validated by γ-secretase specific inhibitor L-685,458 (10 μM, Calbiochem).

[20]. We tested whether β-arrestin1 might likewise modulate γ-secretase activity in a protein-protein interaction-dependent manner. At least four components, PS, NCT, APH-1 and PEN-2, are required for γ-secretase proteolytic activity [9, 10]. We incubated [^{35}S]-labeled β-arrestin1 with immobilized PS1-NTF, PS1-CTF, NCT, APH1-AL or PEN-2. We found that β-arrestin1 bound to APH1-AL but not other γ-secretase components, as revealed by autoradiography (Figure 2A), indicating a direct interaction between β-arrestin1 and APH1-AL. Cellular interactions between β-arrestin1 and γ-secretase components were examined by co-immunoprecipitation (Co-IP) assay. HA-β-arrestin1 was detected only in the Flag-tagged APH1-AL immunopurified complex (Figure 2B). This Co-IP was achieved in Triton X-100 extracts (i.e., under conditions disrupting the associations among γ-secretase components) [21], underscoring the specificity of the β-arrestin1/APH1-AL interaction. Confocal microscopy images showed that β-arrestin1 and APH1-AL exhibited punctate distributions with substantial colocalization within cytoplasm and formed clusters in the perinuclear organelles (Figure 2C), suggesting the association of β-arrestin1 and APH1-AL in intact cells. Moreover, we observed the interaction of β-arrestin1 with APH1-B, a homolog of APH1-AL, but not with APH1-AS, a short alternative splicing variant of APH1-AL lacking the C-terminal extension (Figure 2D). We did not detect any interaction between β-arrestin1 and either APP or BACE1, the other two key proteins involved in Aβ production (Supplementary information, Figure S2A). To test whether cellular signals cause dynamic changes in the β-arrestin1/APH1-AL interaction, we examined the effect of activation of β_2-AR (Gαs coupled GPCR), DOR (Gαi coupled GPCR) and Angiotensin II receptor (Gαq coupled GPCR) on the association of β-arrestin1 and APH1-AL by Co-IP. We found that activation of β_2-AR, DOR and Angiotensin II receptor with their agonists isoproterenol, DADLE and Angiotensin II had little effect on the β-arrestin1/APH1-AL interaction as assayed by Co-IP (Supplementary information, Figure S2B).

Next, we screened for APH-1 binding-deficient mutants of β-arrestin1. We applied a series of β-arrestin1 mutants in the Co-IP assay (Supplementary information, Figure S2C). The γ-secretase activities in the presence of wild-type β-arrestin1 or the mutants were measured in parallel (Supplementary information, Figure S2D). We found that a β-arrestin1 fragment comprised of residue 241 to 360 bound to APH1-AL and augmented γ-proteolytic activity similarly to wild-type β-arrestin1. Further screening showed that β-arrestin1 8M, a β-arrestin1 point mutant harboring the R282A, E283A, K284A and R285A mutations, weakly bound to either APH1-AL or APH1-B (Figure 2E and 2F) and had little effect on the γ-secretase activity (Figure 2G). β-Arrestin1 8M still maintained the normal function of β-arrestin1, as assessed by its binding to GPCRs (Supplementary information, Figure S2E) and translocation into clusters upon β_2-AR activation (Supplementary information, Figure S2F). Interestingly, we found that overexpression of wild-type β-arrestin1 or β-arrestin1 8M had little effect on NotchΔE processing (Figure 2H). To further assess the effect of β-arrestin1 on different γ-secretase substrates, a previously reported sensitive and quantitative reporter gene assay was applied [22]. As shown in Supplementary information, Figure S2G, overexpression of wild-type β-arrestin1 but not β-arrestin1 8M could enhance the cleavage of C99, which is the direct substrate of γ-secretase generated by BACE-cleaved APP. On the other hand, overexpression of wild-type β-arrestin1 or β-arrestin1 8M did not affect the cleavage of NotchΔE. Moreover, another γ-secretase substrate E-cadherin was used to test the β-arrestin1 effect on γ-secretase activity. As shown in Supplementary information, Figure S2H, overexpression of wild-type β-arrestin1 or β-arrestin1 8M had little effect on E-cadherin processing by γ-secretase. Collectively, all these results suggest that the regulation of γ-secretase by β-arrestin1 may be specific for APP proteolysis.

Interference of β-arrestin1/APH-1 interaction reduces Aβ production

We synthesized peptides corresponding to the cytoplasmic loops and C-terminus of APH1-AL and APH1-B (Figure 3A, sequences were shown in Supplementary information, Figure S3A). All peptides were labeled by FITC and tagged with the 11-residue-TAT-tag that has been shown to deliver peptides into many types of living cells [23] (Supplementary information, Figure S3B). No significant cell toxicity of these peptides was observed. We treated cells overexpressing β-arrestin1 and APH1-AL (Figure 3B) or APH1-B (Figure 3C) with the indicated FITC/TAT-tagged peptide, and found that the interaction between β-arrestin1 and APH1-AL was blocked by the C-terminus of both APH1-AL and APH1-B (ACT and BCT), but not by those cytoplasmic loops (Figure 3B). Similar result was obtained in β-arrestin1/APH1-B interaction (Figure 3C), indicating that binding of β-arrestin1 with APH-1 depends on APH-1 C-terminus, and β-arrestin1 might bind to APH1-AL or APH1-B C-terminus via the same domain in β-arrestin1. These are consistent with our observation that β-arrestin1 does not bind to the APH1-AS (Figure 2D). We then treated APPswe HEK293 cells (HEK293 cells stably express-

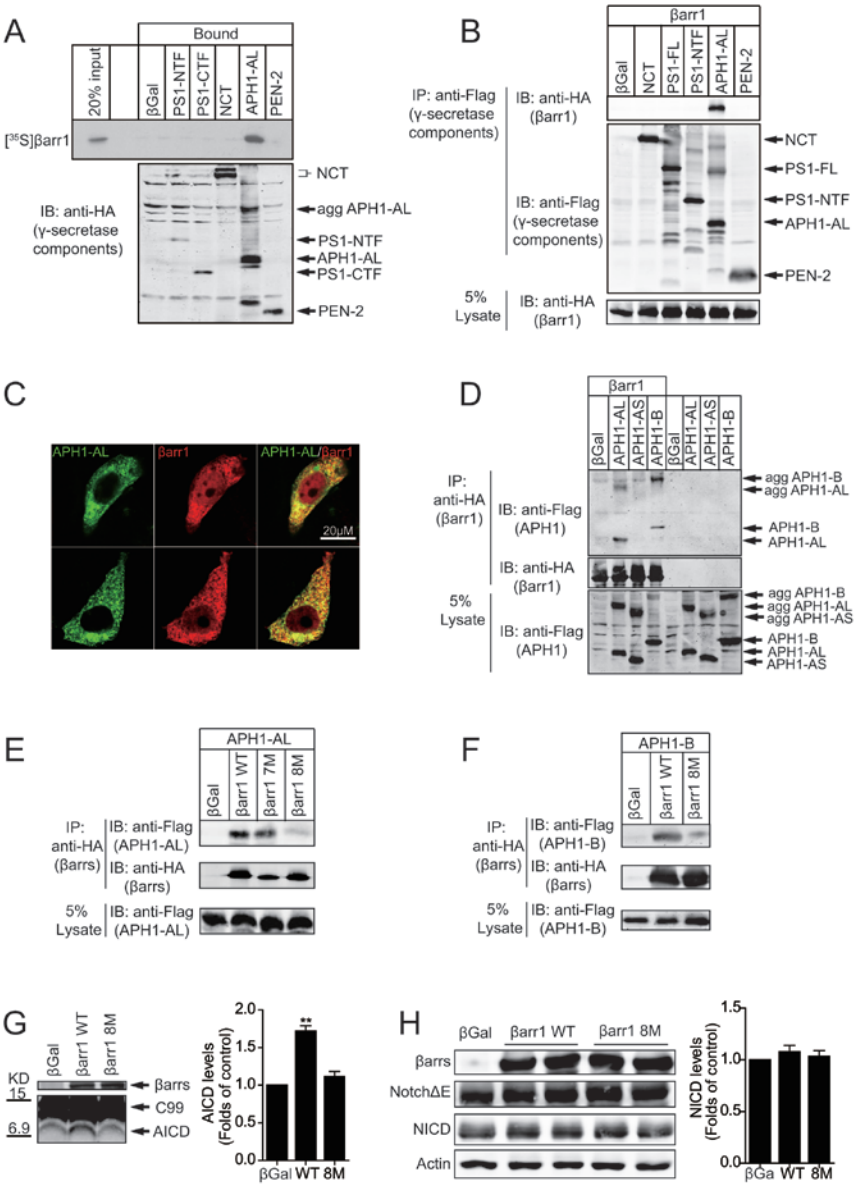

Figure 2 β-Arrestin1 enhances γ-secretase activity via its interaction with APH-1. **(A)** β-arrestin1 directly interacts with APH1-AL. HA-tagged PS1-NTF, PS1-CTF, NCT, APH1-AL and PEN-2 were immunopurified from HEK293T cells with anti-HA resins. Equal amount of ^{35}S-labeled β-arrestin1 protein was incubated with the immobilized proteins (as shown in the lower panel). The bound β-arrestin1 was detected by autoradiography (upper panel). **(B)** β-arrestin1 interacts with APH1-AL but not other γ-secretase components. Triton X-100 extracts of HEK293T cells overexpressing Flag-tagged PS1-FL, PS1-NTF, NCT, APH1-AL or PEN-2 along with HA-tagged β-arrestin1 were subjected to Co-IP assay using anti-Flag resins. **(C)** Immunofluorescence analysis showed the β-arrestin1/APH1-AL colocalization. HEK293 cells were stained with FITC-conjugated anti-HA antibody and Cy3-conjugated anti-Flag antibody to probe overexpressed HA-tagged APH1-AL (green) and Flag-tagged β-arrestin1 (red). Scale bar represents 20 μm. **(D)** Co-IP shows the interaction between β-arrestin1 and APH-1 isoforms. β-Arrestin1 interacts with APH1-AL and APH1-B, but not APH1-AS. **(E**, **F)** APH1-AL **(E)** and APH1-B **(F)** interacts with wild-type (WT) β-arrestin1 but not the β-arrestin1 8M point mutant. Triton X-100 extracts of HEK293T cells overexpressing βGal, HA-tagged β-arrestin1 WT, β-arrestin1 7M (256-261 6Ala) or β-arrestin1 8 M (282-285 4Ala) along with Flag-tagged APH-1 were subjected to Co-IP. **(G)** C99 assay. Equal amount of microsomal membrane fractions of HEK293T cells overexpressing βGal, β-arrestin1 WT or β-arrestin1 8M point mutant was subjected to *in vitro* γ-secretase assay. γ-secretase activity was reflected by production of AICD. **(H)** Notch processing is not affected by overexpression of β-arrestin1 or β-arrestin1 8M. Lysates of HEK293 cells overexpressing βGal, HA-tagged β-arrestin1 WT or HA-tagged β-arrestin1 8M along with Myc-tagged NotchΔE were subjected to SDS-PAGE, immunoblotted by the indicated antibodies. The generation of NICD represented the Notch-specific γ-secretase activity.

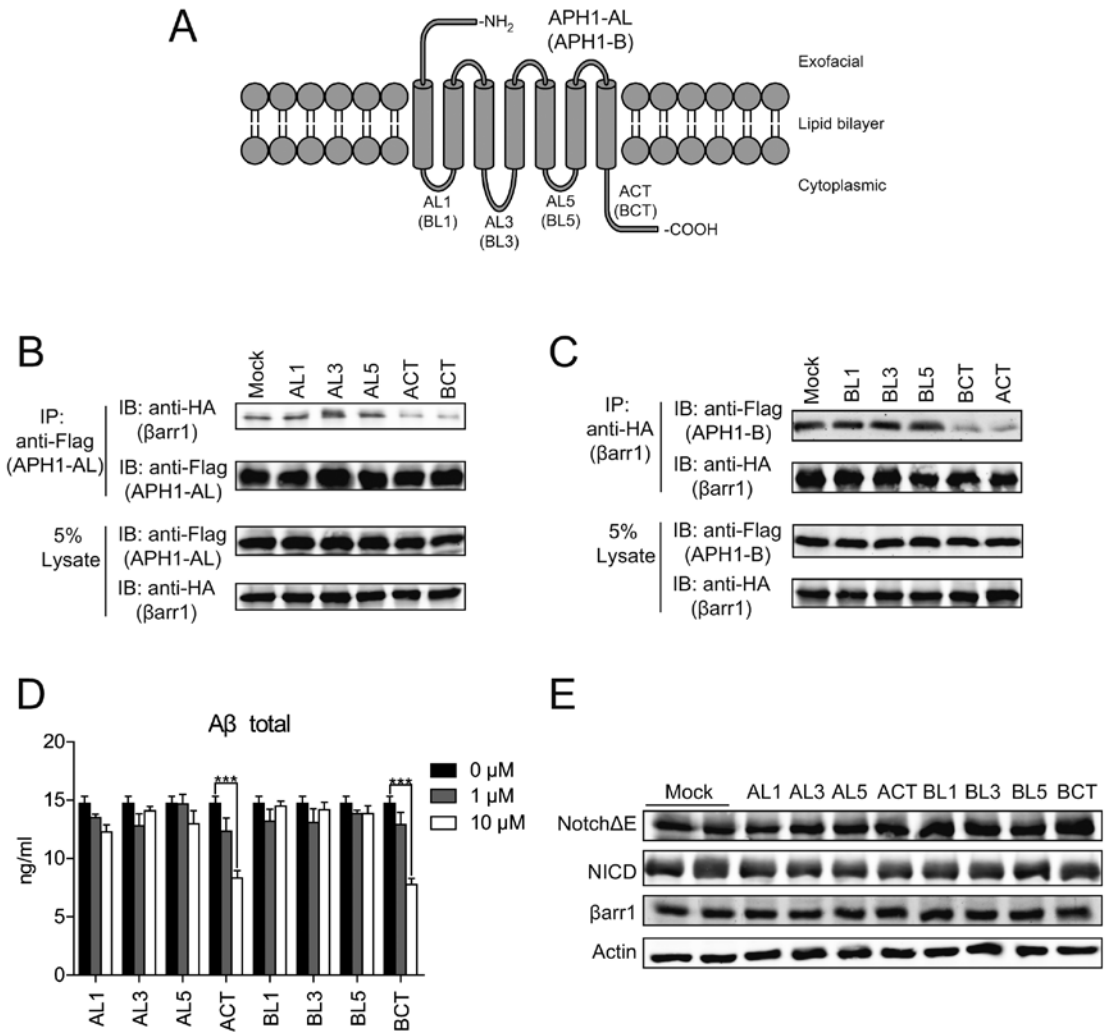

Figure 3 Interference of β-arrestin1/APH-1 interaction reduces Aβ production. **(A)** Schematic plot of the TAT-tagged peptides corresponding to the cytoplasmic loops and C-terminus of APH1-AL and APH1-B. **(B**, **C)** ACT or BCT treatment blocked the interaction between β-arrestin1 and APH1-AL **(B)**, or APH1-B **(C)**. HEK293T cells overexpressing HA-tagged β-arrestin1 and Flag-tagged APH1-AL or APH1-B were treated with 10 μM of the indicated TAT-tagged peptides in the media for 36 h. Mock represented the sample treated by media. Triton X-100 extracts were subjected to Co-IP assay. **(D)** APPswe HEK293 cells were treated with 0, 1 or 10 μM of the indicated TAT-tagged peptides in the media for 36 h. Media were then collected and subjected to ELISA specific for Aβ. Error bars represent SEM. **(E)** Notch processing is not affected by TAT-tagged peptides treatment. HEK293 cells overexpressing Myc-tagged NotchΔE (NΔE) were treated with 10 μM of the indicated TAT-tagged peptides. Cell lysates were then subjected to SDS-PAGE, immunoblotted by the indicated antibodies.

ing APP Swedish mutant) with these peptides. The ACT or BCT treatment did not affect the expression level of either APPswe or the γ-secretase components in APPswe HEK293 cells (Supplementary information, Figure S3C). On the other hand, the Aβ production and γ-secretase (but not α- or β-secretase) activity were significantly reduced by treatment with ACT or BCT but not with other cytoplasmic loops (Figure 3D; Supplementary information, S3D). We further tested the Notch processing in cells treated by these peptides. Cells overexpressing Myc-tagged NotchΔE and treated by any of these eight peptides generated similar amount of NICD compared with controls (Figure 3E). Taken together, our results indicate that inhibition of binding of β-arrestin1 with APH-1 reduces Aβ production and γ-secretase activity.

β-Arrestin1 modulates γ-secretase complex formation via its interaction with APH-1

In the β-arrestin1-knockout mice, we found that β-arrestin1 deficiency had no obvious effect on the ex-

pression level of the γ-secretase components (Supplementary information, Figure S4A). Thus, we examined the potential effect of β-arrestin1 on the γ-secretase complex assembly. In Blue Native-Polyacrylamide Gel Electrophoresis (BN-PAGE), the ~440 KD band represents the mature γ-secretase complex [14, 24]. The supernatants during the membrane preparation (see Supplementary information, Data S1) were subjected to SDS-PAGE (western blot) to ensure the equal loading of membrane protein in each lane (Figure 4A, lower panel). We found that overexpression of β-arrestin1, but not β-arrestin1 8M, facilitated the mature γ-secretase complex formation (Figure 4A), suggesting a β-arrestin1/APH-1 interaction-dependent regulation of γ-secretase complex assembly.

The prevailing view of γ-secretase complex assembly is that the formation of a dimeric NCT/APH-1 intermediate precomplex initiates the assembly, followed by the sequential incorporation of PS and PEN-2 [25-28]. Deficiency of PS abolishes the mature γ-secretase complex formation and its proteolytic activity [29], and induces accumulation of the NCT/APH-1 precomplex [28]. We found that β-arrestin1 did not incorporate into the mature γ-secretase complex, but co-migrated with the about 200 KD NCT/APH-1 precomplex (Figure 4A, arrowed

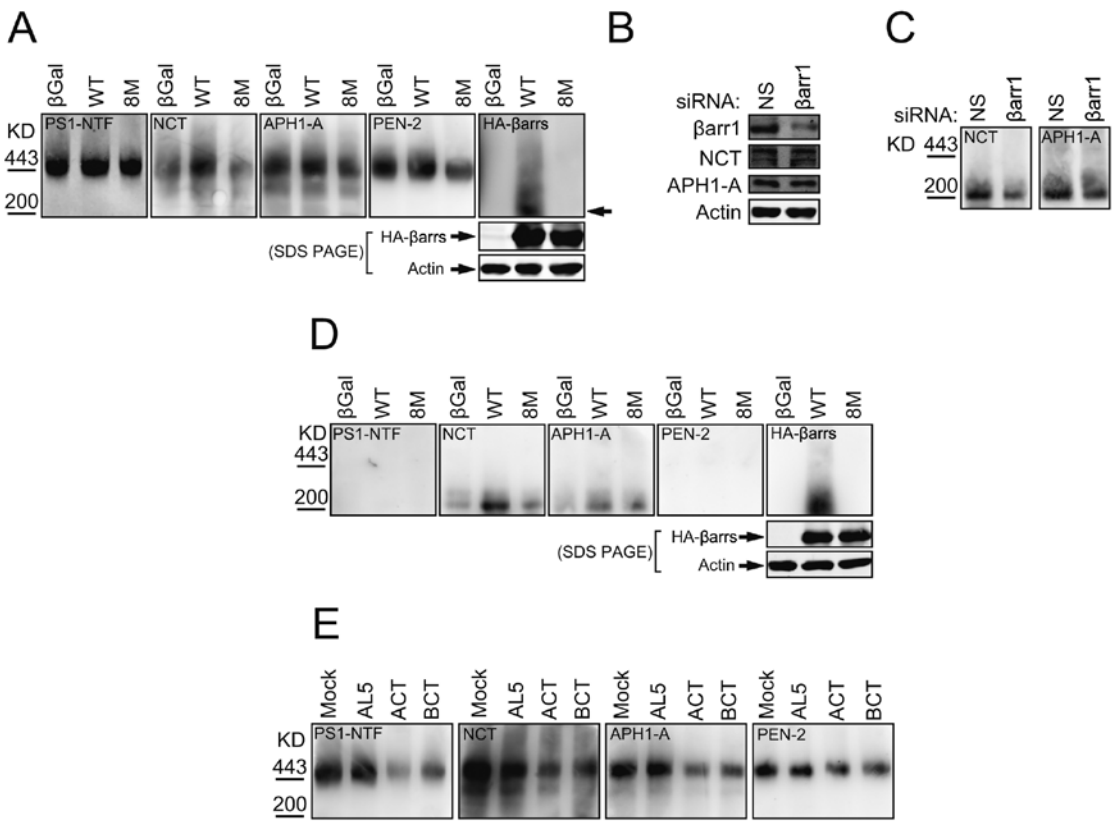

Figure 4 β-Arrestin1 modulates γ-secretase complex formation via its interaction with APH-1. **(A)** HEK293 cells were transfected with βGal, β-arrestin1 WT (WT) or β-arrestin1 8M (8M). During the native extraction of microsomal membrane, after high speed centrifugation the pellets representing the microsomal membranes were subjected to BN-PAGE (0.2% DDM), analyzed by immunoblot using the indicated antibodies against γ-secretase components, whereas the supernatants were subjected to SDS-PAGE and immunoblotted by anti-HA and anti-actin antibodies as loading control. **(B)** Efficient knockdown of β-arrestin1 in PS1/2 double knockout MEF cells by specific siRNA. PS1/2 double knockout MEF cells were transfected with β-arrestin1 specific siRNA or non-specific (NS) control siRNA and were cultured for 96 h. Western blot analysis shows that β-arrestin1 knockdown does not alter the expression level of NCT and APH-1. **(C)** Microsomal membranes of PS1/2 double knockout MEF cells transfected with β-arrestin1 specific siRNA or non-specific (NS) control siRNA were subjected ot BN-PAGE (0.5% DDM). The formation of the NCT/APH-1 precomplex was reduced upon β-arrestin1 knockdown. **(D)** PS1/2 double knockout MEF cells were transfected with βGal, β-arrestin1 WT (WT) or β-arrestin1 8M (8M). BN-PAGE and SDS-PAGE were carried out as **(A)** but with 0.5% DDM. **(E)** HEK293 cells were treated with 10 μM of the indicated TAT-tagged peptides in the media for 36 h. Microsomal membranes were extracted under native conditions and subjected to BN-PAGE (0.2% DDM), analyzed by immunoblot using the indicated antibodies.

bands). This led to our hypothesis that β-arrestin1 might modulate the formation of the mature γ-secretase complex via regulation of the NCT/APH-1 precomplex. In PS 1/2 double knockout mouse embryonic fibroblast (MEF) cells, we did observe that PS deficiency abolished mature γ-secretase complex formation and led to an accumulation of the NCT/APH-1 precomplex (~200 KD band) as reported previously. Further, we found that the NCT/APH-1 precomplex was reduced when β-arrestin1 was knocked down by specific siRNA (Figure 4B and 4C) in the PS 1/2 double knockout MEF cells. However, the expression of NCT and APH-1 were not changed upon β-arrestin1 knockdown. Furthermore, we found that overexpression of β-arrestin1 but not β-arrestin1 8M enhanced the amount of NCT/APH-1 precomplex (Figure 4D). The overexpressed β-arrestin1 but not β-arrestin1 8M co-migrated with the NCT/APH-1 precomplex. These results suggest that β-arrestin1 might facilitate the NCT/APH-1 precomplex assembly and thus mediate γ-secretase holo-complex assembly through its interaction with APH-1. For further verification, the cells treated by ACT or BCT peptides were subjected to BN-PAGE. The formation of NCT/APH-1 precomplex (Supplementary information, Figure S4B) and mature γ-secretase complex (Figure 4E) was decreased in the presence of ACT or BCT. It has been reported that γ-secretase complex assembly is initiated in the early compartments of endoplasmic reticulum (ER) with the formation of the NCT/APH-1 precomplex [30], thus β-arrestin1 is likely to localize to the early compartments. As shown in Supplementary information, Figure S4C, colocalizations between endogenous β-arrestin1 and the ER membrane marker Calnexin were observed. Moreover, as reported previously, suppression of PEN-2 by specific siRNA resulted in inhibition of PS endoproteolysis and accumulation of full-length PS (Supplementary information, Figure S4D) with a trimeric complex containing PS, NCT and APH-1 (Supplementary information, Figure S4E) [9, 31]. However, we could not detect co-migration of β-arrestin1 with this trimeric complex. Taken together, our results suggest that by its interaction with APH-1, β-arrestin1 facilitates the NCT/APH-1 precomplex formation and thus modulates the assembly and activity of γ-secretase.

Genetic ablation of β-arrestin1 ameliorates memory deficits in AD mice

To test whether β-arrestin1 is involved in AD pathogenesis *in vivo*, we crossed APP/PS1 mice [32] with β-arrestin1-knockout mice ($\beta arr1^{-/-}$) [33], and compared the AD-like pathologies of these mice. Detailed mouse information (genotype, sex, age) is shown in Supplementary information, Figure S5A and Table S1. APP/PS1 mice exhibit an aggressive onset of age-dependent neuritic Aβ deposition in the cortex and hippocampus accompanied by memory deficits [14, 34]. We assessed the object exploration and reactivity to object novelty as the reflex of object recognition memory. There were no differences among $\beta arr1^{+/+}$ APP/PS1 mice, $\beta arr1^{-/-}$ APP/PS1 mice, $\beta arr1^{-/-}$ mice and their wild-type littermates ($\beta arr1^{+/+}$) in their object preferrence because the percentage of time spent on exploring each of the two identical objects during training was comparable (Figure 5A). Following a one-hour delay, one of the familiar objects was replaced by a novel object, and the percentage of the time spent on exploring the novel object (recognition index) was measured (Figure 5B). The wild-type mice exhibited a significant increase in time spent on exploring the novel object, compared with the familiar one ($P < 0.0001$). The β-arrestin1-deficient non-AD mice behaved similarly as the wild-type mice (Figure 5B). This observation is consistent with the previous reports that depletion of β-arrestin1 leads to unobvious dysfunction of CNS [33]. In contrast, the APP/PS1 mice did not spend more time on exploring the novel object. Interestingly, the $\beta arr1^{-/-}$ APP/PS1 mice spent more time on exploring the novel object than the familiar one ($P < 0.0001$). One-way ANOVA on the recognition index (Figure 5B) was performed followed by post hoc tests, $P < 0.0001$ ($\beta arr1^{+/+}$ vs $\beta arr1^{+/+}$APP/PS1, $P < 0.001$; $\beta arr1^{+/+}$APP/PS1 vs $\beta arr1^{-/-}$APP/PS1, $P < 0.001$), indicating that the response to object novelty was rescued by ablation of β-arrestin1.

We further used Morris water maze (MWM) to assay the spatial learning and reference memory of these mice. As shown in Figure 5C, during hidden platform testing, APP/PS1 mice exhibited significantly slower learning rates compared with their non-transgenic littermates ($P < 0.001$), indicating consistent learning and memory deficits in APP/PS1 mice, as reported previously. Interestingly, the spatial learning and memory impairment in APP/PS1 mice was ameliorated by the knockout of β-arrestin1 ($\beta arr1^{-/-}$ APP/PS1 vs $\beta arr1^{+/+}$ APP/PS1 mice, $P = 0.0145$). To assess reference memory, we administered a probe trial on day 11. Compared with $\beta arr1^{+/+}$ APP/PS1 mice, the $\beta arr1^{-/-}$ APP/PS1 mice spent more time in the target quadrant where the platform used to be ($P = 0.032$, *t*-test; Figure 5D and 5E). One-way ANOVA on percent time in the target quadrant was also performed followed by post hoc tests, $P = 0.0151$ ($\beta arr1^{+/+}$ mice vs $\beta arr1^{+/+}$ APP/PS1 mice, $P < 0.05$; $\beta arr1^{+/+}$ APP/PS1 mice vs $\beta arr1^{-/-}$ APP/PS1 mice, $P < 0.05$). β-Arrestin1 knockout did not affect the motor ability or motivation of the mice (Figure 5F). Moreover, knockout of β-arrestin1 in non-transgenic

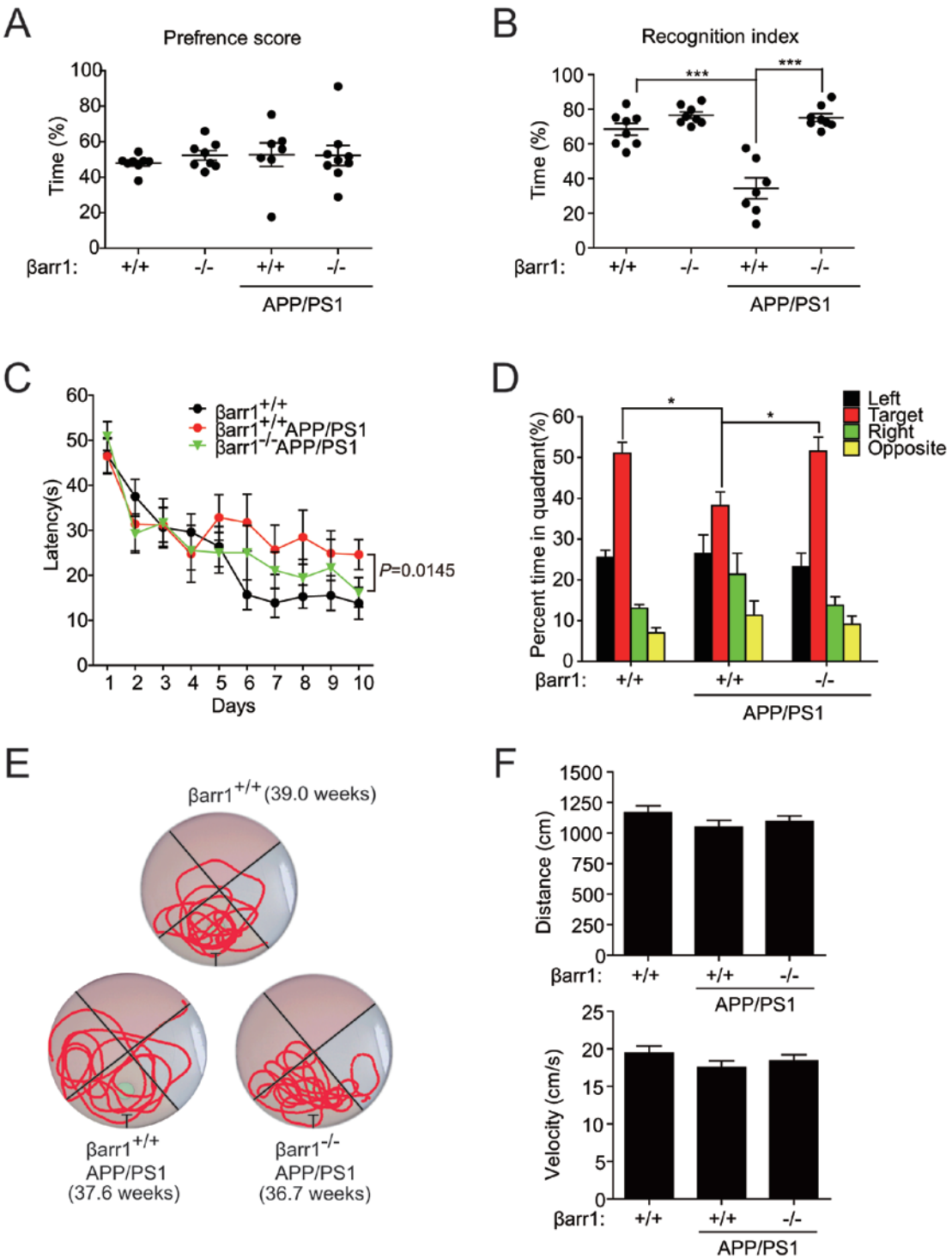

Figure 5 Genetic ablation of β-arrestin1 ameliorates memory deficits in AD mice. **(A**, **B)** The β-arrestin1 deficiency rescues recognition memory deficit in APP/PS1 mice (*n* = 7-9 for each group). Preference score **(A)** was the percentage of time that mice spent on exploring one of the two identical familiar objects in training session; recognition index **(B)** was the time that mice spent on exploring a novel versus a familiar object during a 10 min test session. **(C)** Learning curves during hidden platform training in MWM. The latency of each mouse to reach the hidden platform was recorded. **(D)** Time that took mice to search in the target quadrant in probe trial on day 11 was recorded. **(E)** Representative tracks of each genotype of mice in probe trial on day 11 were shown. "T" represents the target quadrant where the platform used to be. **(F)** The swimming distance (upper panel) and velocity (lower panel) remain unchanged upon APP/PS1 transgene or β-arrestin1 knockout. **P* < 0.05, ****P* < 0.001.

mice ($\beta arr1^{-/-}$ vs $\beta arr1^{+/+}$ mice) leads to undetectable difference in performance of the mice in MWM (Supplementary information, Figure S5B and S5C). These results indicate that the ablation of β-arrestin1 ameliorates the spatial learning and reference memory deficiency of APP/PS1 transgenic mice. Taken together, the genetic ablation of β-arrestin1 significantly ameliorates the AD-like memory deficits in APP/PS1 transgenic mice.

β-Arrestin1 deficiency reduces Aβ production and γ-secretase activity in APP/PS1 mice

After the above behavioral tests, all the mice were sacrificed for further assessment of their AD-like pathology. The APP/PS1 mice exhibited typically elevated Aβ levels and detectable immunofluorescence-positive Aβ deposits, which were markedly reduced in the $\beta arr1^{-/-}$ APP/PS1 mice ($P < 0.05$ vs $\beta arr1^{+/+}$ APP/PS1 mice) (Figure 6A). ELISA analysis further revealed a consistent reduction in the hippocampal and cortical levels of Aβ40 and Aβ42 induced by depletion of β-arrestin1 (Figure 6B). β-Arrestin1 deficiency had no effect on the ratios of soluble or insoluble Aβ42 to Aβ40 in either cortex or hippocampus (Figure 6B, bottom panel). We further measured α-, β- and γ-secretase activities in mouse brain samples. We found that the activity of γ-secretase but not α- or β- secretase was significantly reduced in the $\beta arr1^{-/-}$ APP/PS1 mouse compared with the $\beta arr1^{+/+}$ APP/PS1 mice (Figure 6C). Western blot analysis of the mice brain samples revealed that β-arrestin1 deficiency resulted in the accumulation of both amyloidogenic (CTFβ, C99) and non-amyloidogenic (CTFα, C83) carboxyl-terminal APP fragments without altering the levels of full-length APP, α-secretase (ADAM10), β-secretase (BACE) and γ-secretase components (Figure 6D). We also observed decreased endoproteolysis of PS1 due to the homo-PS1 transgenes as reported previously [32]. The accumulation of C99 and C83 along with the reduction of Aβ levels indicate that the elimination of β-arrestin1 expression reduced γ-secretase activity and amyloid-β pathologies in APP/PS1 transgenic mice.

It is noteworthy that the levels of NICD, the Notch intracellular fragment produced by γ-secretase [35], were indistinguishable among the various mouse genotypes (Figure 6D), suggesting that the expression of β-arrestin1 might specifically regulates APP proteolysis but has little effect on Notch processing, which is consistent with the fact that β-arrestin1-knockout mice exhibit no gross abnormalities [33].

By BN-PAGE, we monitored the γ-secretase complex formation in the brains of β-arrestin1$^{-/-}$ APP/PS1 mice. We found that β-arrestin1 deficiency led to a decrease of relative amount of mature γ-secretase complex in AD mouse brains (Figure 6E). Interestingly, the formation of the mature γ-secretase complex was reduced but not totally blocked upon knockout of β-arrestin1, strongly suggesting that β-arrestin1 might bind with a portion of the NCT/APH-1 precomplex and β-arrestin1 could modulate the γ-secretase complex assembly *in vivo*.

To further confirm our findings that β-arrestin1 depletion results in decreased Aβ levels in AD mice, we intracranially injected lentiviral vectors expressing β-arrestin1 siRNA into the hippocampus of 6-month-old TgCRND8 mice to knockdown endogenous β-arrestin1. Lentiviral vectors encoding siRNA targeting LacZ was applied for nonspecific viral effects. LacZ and β-arrestin1 siRNAs did not have detectable non-target effects on inducing interferon expression in hippocampus (Supplementary information, Figure S6A). Fluorescent images of co-expressed GFP by lentiviral vectors displayed the distribution of these lentiviral vectors in TgCRND8 mouse brains. Four weeks after the stereotaxic injections, both lentiviral vectors were expressed at comparable levels in the bilateral hippocampi (Supplementary information, Figure S6B). The highest expression was observed throughout the dentate gyrus. Immunohistochemical analysis showed that injection of β-arrestin1 siRNA lentivirus remarkably reduced endogenous β-arrestin1 levels. We then probed brain sections with anti-Aβ 6E10 antibody to detect amyloid plaques. We observed a significant reduction of 6E10-positive amyloid plaques in the hippocampus that received β-arrestin1 siRNA compared to that received LacZ siRNA. No significant change was found in other brain regions such as the cortex, where no lentiviral vector was delivered. Morphometric analysis confirmed that knockdown of β-arrestin1 significantly reduced amyloid plaques in the hippocampus, but not in the cortex (Supplementary information, Figure S6C). These results suggest that knockdown of β-arrestin1 decreased Aβ levels in AD mice.

By using cDNA microarrays, Bossers *et al*. [16] reported the gene expression profiles of postmortem brain samples of AD patients at various Braak stages [5]. Interestingly, Bossers *et al*. reported that more senile amyloid plaques were detected in brains of patients with higher Braak stages and the senile amyloid burden correlated well with the Braak stage [16]. Thus we further explored this cDNA microarray data to identify whether there could be a coincidence between the expression of β-arrestin1 and AD pathology. Interestingly, we found a correlation between the Braak stage and the mRNA level of β-arrestin1 (Supplementary information, Figure S6D), but not β-arrestin2 (Supplementary information, Figure S6E). Densitometric analysis of western blots using the same human brain samples provided by

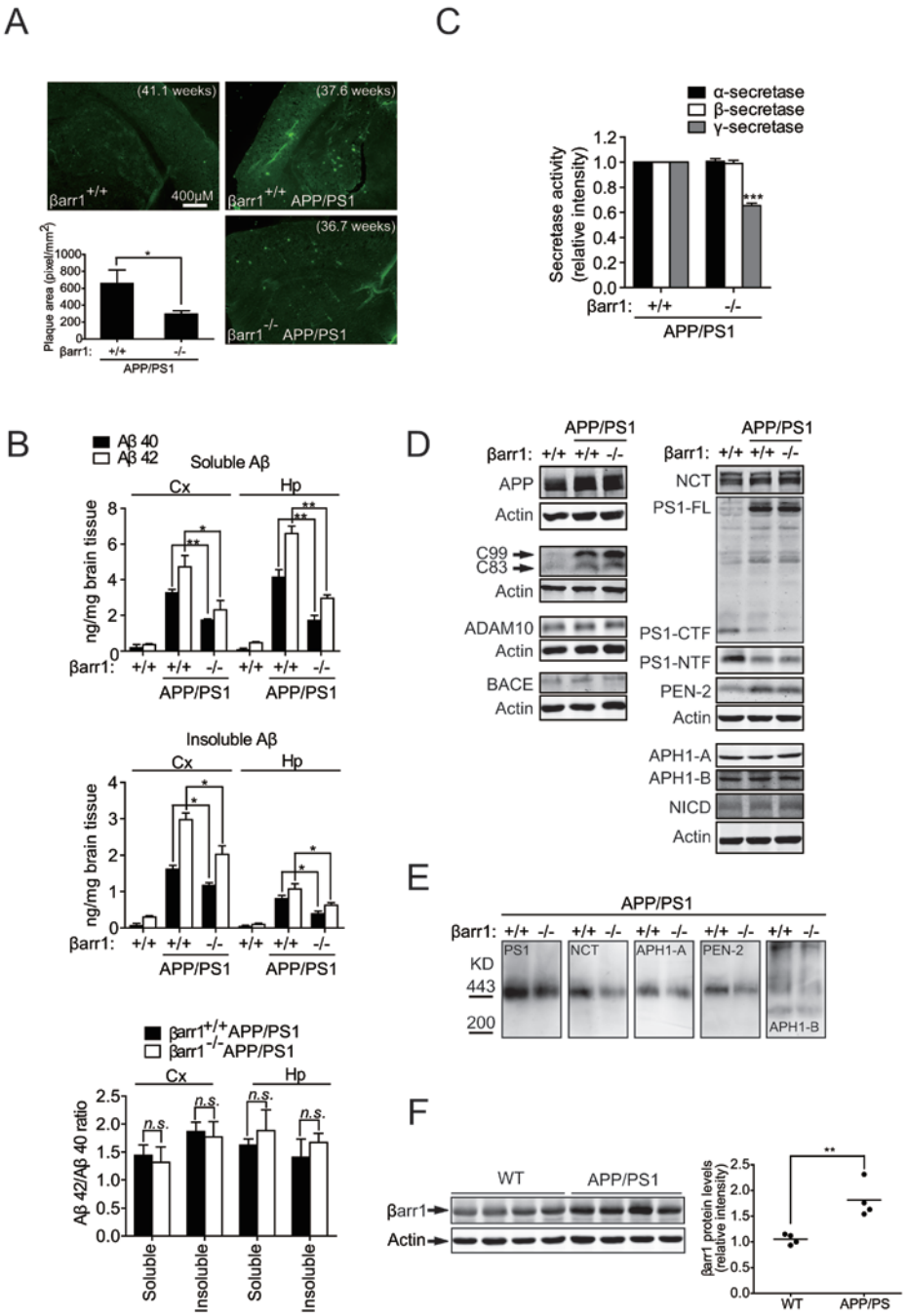

Figure 6 β-Arrestin1 deficiency reduces Aβ production and γ-secretase activity in APP/PS1 mice. **(A)** Reduced amyloid-β plaque in βarr1$^{-/-}$ APP/PS1 mice was revealed by immunostaining with Aβ antibody 6E10 in coronal mouse brain ice sections (representative sections shown, measured by Image-Pro Plus 5.1, n = 4-5 for each group, $P < 0.05$). **(B)** Soluble and insoluble Aβ40 and Aβ42 in mice cortex (Cx) and hippocampus (Hp) were measured by Aβ40 or Aβ42 specific ELISA kit (upper and middle panel, n = 4-5 for each group, $^{*}P < 0.05$, $^{**}P < 0.01$). Aβ abundance was normalized to wet brain tissue weight. The Aβ42 to Aβ40 ratio remained unchanged upon β-arrestin1 knockout in APP/PS1 mice (lower panel, n.s., not significant). **(C)** Activities of α-, β-, and γ-secretase in hippocampal extracts of βarr1$^{+/+}$ APP/PS1 and βarr1$^{-/-}$ APP/PS1 mice were determined by specific fluorogenic substrate assay (n = 4 for each group). $^{***}P < 0.001$. **(D)** Western blot analysis of hippocampal protein extracts of βarr1$^{+/+}$, βarr1$^{+/+}$ APP/PS1 and βarr1$^{-/-}$ APP/PS1 mice with the indicated antibodies. **(E)** Brain samples from βarr1$^{+/+}$ APP/PS1 and βarr1$^{-/-}$ APP/PS1 mice were extracted under native conditions and subjected to BN-PAGE, analyzed by immunoblot using the indicated antibodies. β-Arrestin1 knockout reduces the amount of the mature γ-secretase complex. **(F)** Western blot analysis of β-arrestin1 in APP/PS1 mice hippocampal protein extracts. The APP/PS1 mouse aged from 7-8 months.

Bossers *et al*. also showed that the β-arrestin1 protein level correlated well with the Braak stage ($r = 0.725$, $P < 0.001$; Supplementary information, Figure S6F and S6G). β-Arrestin1 level increased significantly in more advanced Braak stages (stage IV, $P = 0.0078$; stage V, $P = 0.017$; stage VI, $P < 0.001$). β-Arrestin2 protein level also correlated with the Braak stage but to a less extent ($r = 0.508$, $P < 0.001$; Supplementary information, Figure S6H). These suggest a potential correlation between the expression of β-arrestin1 and amyloid loading in patients. We also measured β-arrestin1 protein level in brains of two AD transgenic models, APP/PS1 and TgCRND8 mouse [36]. The expression of β-arrestin1 significantly increased in APP/PS1 mouse brains (Figure 6F) and TgCRND8 mice brains (Supplementary information, Figure S6I). Together, these results indicate a correlation between β-arrestin1 and AD pathogenesis, suggesting that β-arrestin1 plays a role in AD pathological progression *in vivo*.

Discussion

Here, we provide evidence that the multifunctional signaling protein β-arrestin1 is involved in AD pathogenesis. β-Arrestin1 enhances γ-proteolysis of APP via its direct interaction with APH-1, thereby modulating Aβ production both *in vitro* and *in vivo*. The correlation between β-arrestin1 level and the pathological severity of AD (senile amyloid plaques) in AD patients' brains further suggests the regulatory function of β-arrestin1 during AD pathogenesis. Our findings should be intriguing because elimination or partial reduction of β-arrestin1 expression is well tolerated, and the mice lacking β-arrestin1 are viable and exhibit no gross abnormalities [33]. Moreover, our study shows that elimination or partial reduction of β-arrestin1 ameliorates Aβ pathological features without completely inhibiting γ-secretase activity or affecting Notch processing, which indicates a preservation of the normal physiological functions of γ-secretase.

We reported here that β-arrestin1 facilitates the formation of the NCT/APH1 precomplex and eventually the mature γ-secretase complex. However, in light of the multifunction of β-arrestin1, this should not be the only mechanism by which β-arrestin1 functions in AD pathogenesis. Further investigation using β-arrestin1 tissue-specific knockout mice should give us a more detailed picture on the regulatory roles of β-arrestin1 in AD progression. Of note, our findings that the mature γ-secretase complex modulated by the β-arrestin1 is specific for APP processing but not Notch or E-cadherin suggest a novel regulatory mechanism underlying the APP proteolytic activity of γ-secretase and AD pathogenesis. Although the precise mechanism by which β-arrestin1 acts as the specific modulator of APP processing is not immediately apparent and how γ-secretase maintains its substrate specificity remains elusive, a generally accepted explanation for the substrate specificity is the differential subcellular localization of γ-secretase complex which may be the morphological basis for substrate and cleavage specificity because protease and its substrates may be secluded in different subcellular compartments or microdomains [30, 37]. As a scaffolding signaling protein, β-arrestin1 may help γ-secretase to locate into subcellular microdomains proper for the APP processing. Using the whole cell-based C99-GVP and NotchΔE-GVP reporter γ-secretase assay, we also observed a β-arrestin1-enhanced γ-secretase activity specific for C99 cleavage but not NotchΔE. Since the "subcellular microdomains" remain undisrupted in the whole cell assay, these findings may provide support for the "subcellular microdomains" speculation. Moreover, our finding that the 241-360 truncate of β-arrestin1 is enough to enhance the γ-secretase activity as wild-type β-arrestin1 may suggest a completely different mechanism from what we have known about β-arrestin1 functions. Nevertheless, truncate mutant of β-arrestin1 together with the APH-1 ACT and BCT peptides thus further provide us with essential tools to unravel the underlying molecular mechanisms by which β-arrestin1 mediates the assembly, activity and subcellular localization of γ-secretase.

According to our findings, β-arrestin1 interacts with APH1 and acts as a positive regulator for the formation of NCT/APH1 precomplex and eventually the mature γ-secretase complex. Interestingly, the Rer1p has been reported to bind with monomeric NCT and compete with APH1 for NCT, thereby negatively regulating the NCT/APH1 precomplex formation in the early compartments [38]. Furthermore, the assembly as well as the activity of γ-secretase can be regulated by GPR3 [14], TMP21 [39]. Therefore, how these γ-secretase regulatory proteins, including β-arrestin1 crosstalk, with each other and function coordinately to mediate the APP processing by γ-secretase should be of great interest and be carefully investigated.

Since various cellular signaling pathways converge at β-arrestins, further investigation may reveal how extracellular stimulus signaling through β-arrestin1 modulate Aβ production. Furthermore, we have shown that interference of β-arrestin1/APH-1 interaction by small peptides could efficiently reduce Aβ production without affecting Notch processing, suggesting that targeting β-arrestin1 and/or its interaction with APH-1

may implicate an appealing avenue for new preventive or therapeutic strategies against AD.

Materials and Methods

Antibodies

Rabbit anti-HA, anti-Flag, anti-NCT, anti-PEN-2, anti-APP-CTF, anti-ADAM10 and anti-Actin antibodies were from Sigma. Rabbit anti-PS1-NTF, anti-PS1-CTF, anti-BACE antibodies were from Calbiochem. Rabbit anti-APH1-AL, anti-APH1-B and anti-Aβ 6E10 antibodies were from Covance. Rabbit anti-NICD (cleaved Notch1 Val-1744) antibody was from Cell Signaling Technologies. Rabbit anti-β-arrestin antibodies (A1CT and A2CT) were provided by Dr Robert J Lefkowitz (Duke University Medical Center, USA).

siRNA sequences

The siRNA sequences for mouse β-arrestin1: sense: 5′-CUGAGAACCUGGAGGAGAATT-3′; anti-sense: 5′-UUCUCCUCCAGGUUCUCAGTT-3′; the siRNA sequences for human Pen-2: sense: 5′-GUACUACCUGGGGGGGUUUTT-3′; anti-sense: 5′-AAACCCCCCCAGGUAGUACTT-3′.

Generation of littermate controlled mice of interested genotypes

The βarr1$^{+/-}$(C3H/C57BL) and APP/PS1$^{+/0}$(hemizygous) (C3H/C57BL) mice were crossed to obtain βarr1$^{+/-}$ APP/PS1$^{+/0}$(C3H/C57BL) mice. The βarr1$^{+/-}$ APP/PS1$^{+/0}$(C3H/C57BL) mice were then crossed with βarr1$^{+/-}$(C3H/C57BL) mice to generate all genotypes of littermate controlled mice used in this study (namely βarr1$^{+/+}$, βarr1$^{-/-}$, βarr1$^{+/+}$APP/PS1 and βarr1$^{-/-}$APP/PS1). Genotyping was performed on genomic DNA by conventional PCR for APP and PS1 transgene (APP primers: 5′-GACTGACCACTCGACCAGGTTCTG-3′, 5′-CTTGTAAGTTGGATTCTCATATCCG-3′; PS1 primers: 5′-GTGGATAACCCCTCCCCCAGCCTAGACC-3′, 5′-AATAGAGAACGGCA GGAGCA-3′) and quantitative real-time PCR for βarr1 genotype (primers: 5′-CCTAGTGCTGGGATTACAAG-3′, 5′-CATAGCCTGAAGAACGAGAT-3′). All mice used in this study were fully genotyped.

Behavioral tests

All behavioral tests were performed by experimenters blinded for mice genotypes. Novelty seeking was performed as previously described [40] with modifications. MWM was performed as previously described [41] with modifications. Full methods are available in Supplementary information, Data S1.

Immunofluorescence microscopy and immunohistochemistry

Cells were fixed with 4% paraformaldehyde and permeabilized with 0.2% Triton X-100. We acquired images by using a confocal fluorescent microscope (Leica TCS SP2 AOBS).

Floating coronal ice sections were incubated with antibody against β-arrestin1 (A1CT, 1:1 000) for 12 h at 4 °C. The slides were then processed using the Vectastain Elite ABC kit (Vector Laboratories) according to the manufacturer's instructions. Images were acquired by using ZEISS OBSERVER Z1 microscope (Carl Zeiss) with AxioCamMR3 digital camera and AxioVision software (Carl Zeiss). Amyloid plaques were quantified with Image-Pro Plus 5.1 software (Media Cybernetic). Full methods are available in Supplementary information, Data S1.

ELISA for Aβ

Endogenous mouse Aβ40 and Aβ42 were extracted as previously reported [42] and measured with BNT77/BA27 and BNT77/BC05 sandwich ELISA kits, respectively. Overexpressed human Aβ40 and Aβ42 in TgCRND8 mice and APP/PS1 mice were extracted as previously reported [43] and were measured with human Aβ40 and Aβ42 ELISA kits (Biosource), respectively; results were expressed in pg/mg wet mice brain tissue.

Fluorogenic substrate assay

We assayed α-, β- and γ-secretase activities by using fluorogenic α-, β- and γ-secretase specific substrates from Calbiochem [44-46]. Cell lysates or brain homogenates were centrifuged at 800× g for 10 min to remove nuclei and cell debris. Microsomal membrane fractions were pelleted from the postnuclear supernatants by centrifugation at 25 000× g for 1 h at 4 °C and were resuspended for reactions. For measuring α-secretase activity, membranes were resuspended in assay buffer containing 10 mM Tris-HCl (pH 7.5) and 20 μM α-substrates (565767, Calbiochem) and incubated at 37 °C for 1 h. For measuring β-secretase activity, reactions were performed in assay buffer containing 50 mM sodium acetate (pH 4.5) and 10 μM β-substrates (565781, Calbiochem) and incubated at 37 °C for 30 min. For measuring γ-secretase activity, reactions were performed in assay buffer containing 50 mM Tris-HCl (pH 6.8), 2 mM EGTA, 150 mM NaCl, 0.25% CHAPSO and 8 μM γ-substrates (565764, Calbiochem) and incubated at 37 °C for 2 h. Fluorescence was determined with a SpectraMax M5 spectrometer (Molecular Devices) and the wavelengths were set for α-substrates (λex = 340 nm; λem = 490 nm), β-substrates (λex = 430 nm; λem = 520 nm) and γ-substrates (λex = 355 nm; λem = 440 nm), respectively.

In vitro cell free γ-secretase assay

The *in vitro* γ-secretase activity assay was performed as previously described [47] with modifications. Full methods are available in Supplementary information, Data S1.

Mouse primary neuronal cultures

For primary neuronal cultures, cortexes from mouse pups were isolated on postnatal day 0 or 1. Dissociated cells were electroporated using Amaxa Nucleofector system and maintained in Neurobasal A medium (Invitrogen) supplemented with B27 (Invitrogen) for 7 days.

BN-PAGE

The BN-PAGE was performed as previously described [14, 24, 48]. The microsomal membranes were extracted in the same way as "Fluorogenic substrate assay". Full methods are available in Supplementary information, Data S1.

Sucrose gradient fractionation

The sucrose gradient subcellular fractionation was performed as previously described [14]. The 45%, 35% and 5% sucrose in MES buffer were chosen to make a discontinuous sucrose gradient. Full methods are available in Supplementary information, Data S1.

Statistical analysis

All results were analyzed with the SigmaStat 3.5 program

(Systat Software). Spearman's correlation coefficient r was calculated to determine the correlations between β-arrestin1/2 levels and Braak stages as well as β-arrestin1 level and age of APP/PS1 mice. Comparisons across Braak groups were obtained using One Way ANOVA analysis with *post-hoc* Student-Newman-Keuls test. The results of MWM hidden platform training were compared using Two Way ANOVA Analysis with *post-hoc* Holm-Sidak test. Data are shown as Mean ± SEM. Data from other *in vitro* and *in vivo* experiments if not addressed were analyzed by Student's *t*-test for comparison of independent means. The null hypothesis was rejected at the 0.05 level.

Acknowledgements

We are grateful to Dr Robert J Lefkowitz for friendly providing us with A1CT and A2CT antibodies, and β-arrestin 1 knockout mice. We thank Dr David Westaway (University of Alberta, Canada) for TgCRND8 mice; Dr Bart De Strooper and Dr Paul Saftig (Katholieke Universiteit Leuven, Belgium) for presenilin knockout MEFs; Dr Harald Steiner (Ludwig Maximilians University, Germany) for APH1-A/B constructs; Dr Robert W Doms (University of Pennsylvania Medical Center, USA) for nicastrin constructs; Dr Sangram S Sisodia (University of Chicago, USA) for PEN-2 constructs. We thank all members of the lab for sharing reagents and advice. This research was supported by the National Natural Science Foundation of China (30871285), Ministry of Science and Technology of China (2011CB910202), Ministry of Health (2012BAI10B03), Shanghai Municipal Commission for Science and Technology (07PJ14099) and Chinese Academy of Sciences (KSCX2-EW-Q-1-01, KSCX2-YW-R-252). JZ was supported by the SA-SIBS Scholarship Program.

References

1 Goedert M, Spillantini MG. A century of Alzheimer's disease. *Science* 2006; **314**:777-781.
2 Amaducci L, Tesco G. Aging as a major risk for degenerative diseases of the central nervous system. *Curr Opin Neurol* 1994; **7**:283-286.
3 Cohen E, Paulsson JF, Blinder P, *et al*. Reduced IGF-1 signaling delays age-associated proteotoxicity in mice. *Cell* 2009; **139**:1157-1169.
4 Ritchie K, Lovestone S. The dementias. *Lancet* 2002; **360**:1759-1766.
5 Braak H, Braak E. Neuropathological stageing of Alzheimer-related changes. *Acta Neuropathol* 1991; **82**:239-259.
6 Hardy J, Selkoe DJ. The amyloid hypothesis of Alzheimer's disease: progress and problems on the road to therapeutics. *Science* 2002; **297**:353-356.
7 Ballatore C, Lee VM, Trojanowski JQ. Tau-mediated neurodegeneration in Alzheimer's disease and related disorders. *Nat Rev Neurosci* 2007; **8**:663-672.
8 Roberson ED, Mucke L. 100 years and counting: prospects for defeating Alzheimer's disease. *Science* 2006; **314**:781-784.
9 Takasugi N, Tomita T, Hayashi I, *et al*. The role of presenilin cofactors in the gamma-secretase complex. *Nature* 2003; **422**:438-441.
10 De Strooper B, Annaert W, Cupers P, *et al*. A presenilin-1-dependent gamma-secretase-like protease mediates release of Notch intracellular domain. *Nature* 1999; **398**:518-522.
11 Blalock EM, Geddes JW, Chen KC, Porter NM, Markesbery WR, Landfield PW. Incipient Alzheimer's disease: microarray correlation analyses reveal major transcriptional and tumor suppressor responses. *Proc Natl Acad Sci USA* 2004; **101**:2173-2178.
12 Teng L, Zhao J, Wang F, Ma L, Pei G. A GPCR/secretase complex regulates beta- and gamma-secretase specificity for Abeta production and contributes to AD pathogenesis. *Cell Res* 2010; **20**:138-153.
13 Ni Y, Zhao X, Bao G, *et al*. Activation of beta2-adrenergic receptor stimulates gamma-secretase activity and accelerates amyloid plaque formation. *Nat Med* 2006; **12**:1390-1396.
14 Thathiah A, Spittaels K, Hoffmann M, *et al*. The orphan G protein-coupled receptor 3 modulates amyloid-beta peptide generation in neurons. *Science* 2009; **323**:946-951.
15 El Khoury J, Toft M, Hickman SE, *et al*. Ccr2 deficiency impairs microglial accumulation and accelerates progression of Alzheimer-like disease. *Nat Med* 2007; **13**:432-438.
16 Bossers K, Wirz KT, Meerhoff GF, *et al*. Concerted changes in transcripts in the prefrontal cortex precede neuropathology in Alzheimer's disease. *Brain* 2010; **133**:3699-3723.
17 DeWire SM, Ahn S, Lefkowitz RJ, Shenoy SK. Beta-arrestins and cell signaling. *Annu Rev Physiol* 2007; **69**:483-510.
18 Lefkowitz RJ. G protein-coupled receptors. III. New roles for receptor kinases and beta-arrestins in receptor signaling and desensitization. *J Biol Chem* 1998; **273**:18677-18680.
19 Attramadal H, Arriza JL, Aoki C, *et al*. Beta-arrestin2, a novel member of the arrestin/beta-arrestin gene family. *J Biol Chem* 1992; **267**:17882-17890.
20 Grady EF. Cell signaling. Beta-arrestin, a two-fisted terminator. *Science* 2007; **315**:605-606.
21 Wakabayashi T, Craessaerts K, Bammens L, *et al*. Analysis of the gamma-secretase interactome and validation of its association with tetraspanin-enriched microdomains. *Nat Cell Biol* 2009; **11**:1340-1346.
22 Karlstrom H, Bergman A, Lendahl U, Naslund J, Lundkvist J. A sensitive and quantitative assay for measuring cleavage of presenilin substrates. *J Biol Chem* 2002; **277**:6763-6766.
23 Schwarze SR, Ho A, Vocero-Akbani A, Dowdy SF. In vivo protein transduction: delivery of a biologically active protein into the mouse. *Science* 1999; **285**:1569-1572.
24 Nyabi O, Bentahir M, Horre K, *et al*. Presenilins mutated at Asp-257 or Asp-385 restore Pen-2 expression and Nicastrin glycosylation but remain catalytically inactive in the absence of wild type Presenilin. *J Biol Chem* 2003; **278**:43430-43436.
25 Hu Y, Fortini ME. Different cofactor activities in gamma-secretase assembly: evidence for a nicastrin-Aph-1 subcomplex. *J Cell Biol* 2003; **161**:685-690.
26 LaVoie MJ, Fraering PC, Ostaszewski BL, *et al*. Assembly of the gamma-secretase complex involves early formation of an intermediate subcomplex of Aph-1 and nicastrin. *J Biol Chem* 2003; **278**:37213-37222.
27 Fraering PC, LaVoie MJ, Ye W, *et al*. Detergent-dependent dissociation of active gamma-secretase reveals an interaction between Pen-2 and PS1-NTF and offers a model for subunit organization within the complex. *Biochemistry* 2004; **43**:323-333.

28 Capell A, Beher D, Prokop S, *et al*. Gamma-secretase complex assembly within the early secretory pathway. *J Biol Chem* 2005; **280**:6471-6478.
29 Herreman A, Serneels L, Annaert W, Collen D, Schoonjans L, De Strooper B. Total inactivation of gamma-secretase activity in presenilin-deficient embryonic stem cells. *Nat Cell Biol* 2000; **2**:461-462.
30 De Strooper B, Annaert W. Novel research horizons for presenilins and gamma-secretases in cell biology and disease. *Annu Rev Cell Dev Biol* 2010; **26**:235-260.
31 Bammens L, Chavez-Gutierrez L, Tolia A, Zwijsen A, De Strooper B. Functional and topological analysis of Pen-2, the fourth subunit of the gamma-secretase complex. *J Biol Chem* 2011; **286**:12271-12282.
32 Jankowsky JL, Slunt HH, Ratovitski T, Jenkins NA, Copeland NG, Borchelt DR. Co-expression of multiple transgenes in mouse CNS: a comparison of strategies. *Biomol Eng* 2001; **17**:157-165.
33 Conner DA, Mathier MA, Mortensen RM, *et al*. beta-Arrestin1 knockout mice appear normal but demonstrate altered cardiac responses to beta-adrenergic stimulation. *Circ Res* 1997; **81**:1021-1026.
34 Serneels L, Van Biervliet J, Craessaerts K, *et al*. gamma-Secretase heterogeneity in the Aph1 subunit: relevance for Alzheimer's disease. *Science* 2009; **324**:639-642.
35 Jorissen E, De Strooper B. Gamma-secretase and the intramembrane proteolysis of Notch. *Curr Top Dev Biol* 2010; **92**:201-230.
36 Dudal S, Krzywkowski P, Paquette J, *et al*. Inflammation occurs early during the Abeta deposition process in TgCRND8 mice. *Neurobiol Aging* 2004; **25**:861-871.
37 Kaether C, Schmitt S, Willem M, Haass C. Amyloid precursor protein and Notch intracellular domains are generated after transport of their precursors to the cell surface. *Traffic* 2006; **7**:408-415.
38 Spasic D, Raemaekers T, Dillen K, *et al*. Rer1p competes with APH-1 for binding to nicastrin and regulates gamma-secretase complex assembly in the early secretory pathway. *J Cell Biol* 2007; **176**:629-640.
39 Chen F, Hasegawa H, Schmitt-Ulms G, *et al*. TMP21 is a presenilin complex component that modulates gamma-secretase but not epsilon-secretase activity. *Nature* 2006; **440**:1208-1212.
40 Bevins RA, Besheer J. Object recognition in rats and mice: a one-trial non-matching-to-sample learning task to study 'recognition memory'. *Nat Protoc* 2006; **1**:1306-1311.
41 Vorhees CV, Williams MT. Morris water maze: procedures for assessing spatial and related forms of learning and memory. *Nat Protoc* 2006; **1**:848-858.
42 Rozmahel R, Huang J, Chen F, *et al*. Normal brain development in PS1 hypomorphic mice with markedly reduced g-secretase cleavage of bAPP. *Neurobiol Aging* 2002; **23**:187-194.
43 Oddo S, Caccamo A, Green KN, *et al*. Chronic nicotine administration exacerbates tau pathology in a transgenic model of Alzheimer's disease. *Proc Natl Acad Sci USA* 2005; **102**:3046-3051.
44 Ni Y, Zhao X, Bao G, *et al*. Activation of b2-adrenergic receptor stimulates g-secretase activity and accelerates amyloid plaque formation. *Nat Med* 2006; **12**:1390-1396.
45 Komano H, Seeger M, Gandy S, Wang GT, Krafft GA, Fuller RS. Involvement of cell surface glycosyl-phosphatidylinositol-linked aspartyl proteases in a-secretase-type cleavage and ectodomain solubilization of human Alzheimer b-amyloid precursor protein in yeast. *J Biol Chem* 1998; **273**:31648-31651.
46 Gruninger-Leitch F, Schlatter D, Kung E, Nelbock P, Dobeli H. Substrate and inhibitor profile of BACE (b-secretase) and comparison with other mammalian aspartic proteases. *J Biol Chem* 2002; **277**:4687-4693.
47 Kakuda N, Funamoto S, Yagishita S, *et al*. Equimolar production of amyloid beta-protein and amyloid precursor protein intracellular domain from beta-carboxyl-terminal fragment by gamma-secretase. *J Biol Chem* 2006; **281**:14776-14786.
48 Wittig I, Braun HP, Schagger H. Blue native PAGE. *Nat Protoc* 2006; **1**:418-428.

(**Supplementary information** is linked to the online version of the paper on the *Cell Research* website.)

SOME RIGHTS RESERVED This work is licensed under the Creative Commons Attribution-NonCommercial-No Derivative Works 3.0 Unported License. To view a copy of this license, visit http://creativecommons.org/licenses/by-nc-nd/3.0